AD-A280 975 ΓATION PAGE

1. AGENCY USE ONLY (Leave blank)	2. REPORT DATE 6 / 20 / 94	3. REPORT TYPE AND DATES COVERED Technical Report

4. TITLE AND SUBTITLE

The Effect of Brush Polydispersity on the Interphase Between End-Grafted Brushes and Polymeric Matrices

5. FUNDING NUMBERS

N00014-91-J-1786

6. AUTHOR(S)

Charles F. Laub and Jeffery T. Koberstein

7. PERFORMING ORGANIZATION NAME(S) AND ADDRESS(ES)

Dept. of Chemical Engineering and Institute of
    Materials Science
University of Connecticut
Storrs, CT 06269-3136

8. PERFORMING ORGANIZATION REPORT NUMBER

9. SPONSORING/MONITORING AGENCY NAME(S) AND ADDRESS(ES)

10. SPONSORING/MONITORING AGENCY REPORT NUMBER

11. SUPPLEMENTARY NOTES

12a. DISTRIBUTION/AVAILABILITY STATEMENT

12b. DISTRIBUTION CODE

13. ABSTRACT (Maximum 200 words)

A self-consistent computer simulation has been used to calculate the concentration profile of an end-tethered polymer chain in a polymer matrix in order to investigate the influence of brush polydispersity on the width of the interphase. It was found that increasing the brush polydispersity increased the width of the interphase between the brush and the matrix. The results suggest that highly polydisperse brushes will result in increased adhesion when compared with an analogous brush of narrow molecular weight distribution.

101 1994

DTIC QUALITY INSPECTED 6

14. SUBJECT TERMS

polymer, brush, molecular weight distribution, adhesion, computer simulation

15. NUMBER OF PAGES
38

16. PRICE CODE

17. SECURITY CLASSIFICATION OF REPORT	18. SECURITY CLASSIFICATION OF THIS PAGE	19. SECURITY CLASSIFICATION OF ABSTRACT	20. LIMITATION OF ABSTRACT
Unclassified	Unclassified	Unclassified	UL
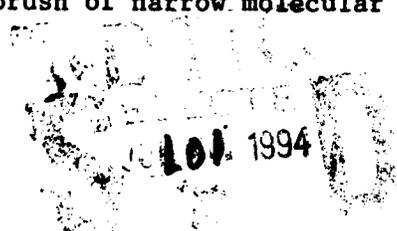
Office of Naval Research

The Effect of Brush Polydispersity on the Interphase Between End-Grafted Brushes and Polymeric Matrices

by Charles F. Laub and Jeffery T. Koberstein

Dept. of Chemical Engineering and Institute of Materials Science
University of Connecticut, Storrs, CT 06269-3136

94-20214

94 6 30 039

Abstract

The effect of polydispersity on the width of the interphase between an end-tethered polymer and a polymeric matrix has been investigated using a computer program which solves a self-consistent field model of a polymer chain distributed on a cubic lattice. This model was used to calculate an average volume fraction of each species along the axis perpendicular to the grafting plane. A Flory-Huggins type expression, generalized to a multicomponent system, was used to model the free energy change of mixing. The logarithmic-normal molecular weight distribution function was employed to generate the desired molecular weight distribution for the end-tethered polymer while the matrix was assumed to be monodisperse. Brushes having polydispersities from 1.0 (monodisperse) to 3.0 were studied under repulsive, attractive and athermal enthalpic brush-matrix interactions. The effect of polydispersity on the width of the interphase was found to be dependent upon the type of enthalpic interaction. When a repulsive brush-matrix interaction existed, the width of the interphase was not affected by brush polydispersity, however the brush profile showed evidence of an increased stretching of the brush into the matrix as the polydispersity was increased from 1.0 to 3.0, indicating enhanced mixing in the interphase. The use of polydisperse brushes at solid-polymer interfaces for adhesion promotion is discussed by considering how enhanced brush-matrix contact and a surface exclusion zone affect the interfacial toughness.

Introduction

It has long been known that the configuration of a polymer near an adsorbing surface is very different than the configuration of a free chain. One interesting and potentially useful configuration adopted by polymers adsorbed at a solid surface is that of a polymer "brush". The term brush describes the structure which arises when the polymer chains are tethered to a surface, line or point by a segment (such as an endgroup) or segments (such as one block of a copolymer). Since some segments are bound to the surface, the rest of the chain is displaced away from it into the medium which the brush is in contact with. The average surface, or grafting density of adsorbed segments largely determines the degree to which the chain is elongated perpendicular to the grafting plane. Many different examples of brush structures exist. A Langmuir-Blodgett film is a brush of oligomeric molecules at very high grafting density. A diblock copolymer which bridges two immiscible polymer phases can be considered to be two-sided brush in which the grafting "surface" is that region where the junction points of the blocks are located. Sterically stabilized colloidal dispersions and micelles can also be considered to be brushes grafted to the surface of a sphere.

While brush structures are employed in such fields as tribology, biophysics, flocculation and colloid stabilization, the focus of this study is on their use as adhesion promoters at the polymer-solid interface. From this point on we shall use the term "brush" to denote a structure consisting of polymer chains which are end-tethered to a flat, smooth surface. A typical example is a so-called silane coupling agent used to reinforce the interphase between a glass fiber and the matrix material in a composite. Studies have demonstrated the importance of good fiber-matrix adhesion on the performance of model composites.[1-4] In the adhesion of a polymer to a surface,

the behavior of the solid-brush interface and interphase are both important. Here we shall refer to the interface as the surface of the solid where the brush chains are bonded or adsorbed. The interphase shall refer to that region in which the transition from the brush phase to the matrix phase is gradual, occurring for the most part over a few nanometers. One would like both to increase the ultimate strength of the interphase as well as the strain before break, so that the toughness of the interphase in increased. Dissipation mechanisms which arise from chain pull-out have been shown to play an important role in the strength of adhesive bonds.[5-7] Of specific interest are recent results of several authors on the adhesion of elastomers to solids.[8-10] Chain pull-out can only occur if the brush and matrix polymer chains are sufficiently entangled throughout the interphase region. The degree of entanglement should be proportional to the width of the interphase and to the relative concentrations of brush and matrix chains across the interphase. Thus, an increase in the width of the brush-matrix interphase will enhance chain entanglement, increase energy dissipation during fracture and lead to a tougher interphase.

Early theoretical investigations of brushes[11-13] explored the basic shape of the concentration profile while more recent papers have dealt with increasingly complex situations (polymeric matrices[14], interface geometry[15], behavior under shear or compression[16]). Most have neglected the fact that polymeric materials have a distribution of molecular weights and thus are not "pure" materials. Only recently has research into the behavior of bidisperse or polydisperse brushes been undertaken.[17,18] It has been demonstrated[17] that the properties of a bidisperse brush may be very different from those of a monodisperse brush. Dramatic changes in the shape of the brush concentration profile have also been observed.[17] A more systematic investigation of

polydisperse brushes in terms of adhesive properties was seen as a natural extension of these studies, and is the objective of this paper.

Theory

In order to study the effect of polydispersity on the width of the interphase a model system must be constructed. We wish to simulate a brush of arbitrary polydispersity, grafting density and degree of polymerization and to include enthalpic interactions between the brush and matrix. The chains are modeled as a series of freely jointed Kuhn segments. The brush is tethered at one end only and the adsorption energy is assumed to be infinite. We assume that the brush structures under study have already been formed by some means and that no brush chains exist in the matrix phase. No other interactions exist between the chain backbone and the grafting surface for both the brush and matrix chains, however interactions may exist between brush and matrix chains. Of primary interest are compositional changes occurring perpendicular to the grafting surface, which is assumed to be a perfectly flat infinite plane. For this reason, the system is assumed to be isotropic in directions parallel to the grafting plane. Furthermore, the interphase is assumed to be diffuse such that any fluctuations are much larger than the dimensions of an unperturbed chain. The above simplifications and restrictions result in a system in which the features of interest may be described by a simple mathematical model.

Let us now concern ourselves with the numerical construction of the system just discussed. The numerical self-consistent mean field treatment used here was pioneered by Cosgrove et. Al.[19] and closely follows the form given by Shull.[14,20] Consider a polymer chain distributed on a cubic lattice in space as shown in Figure 1. There are six "nearest-neighbors" for

3

each coordinate of the lattice. If we are at some segment, j, along the polymer chain, the next segment, j+1, may be located only at one of the nearest neighbor sites. These points determine the connectivity of the chain on the lattice. Since the brush structure is assumed to be isotropic in all directions except for the direction normal to the grafting plane, the four nearest neighbor positions which are in the same lattice layer are equivalent as illustrated in Figure 1. In reality, a polymer chain would have a non-uniform density profile in directions other than that perpendicular to the grafting surface. Recent work has shown that the interphase resembles a rippled surface rather than a purely diffuse interface.[21,22] The perpendicular direction is of primary interest, however, and the one-dimensional lattice simplifies the system considerably.

The central quantities which describe the location of chain segments across the lattice are the "chain probability distribution functions" (PDF), $q(i,j,k)$. Within this discussion, index "i" will always refer to the lattice layer, index "j" the chain segment while index "k" will identify the polymer chain. For each $q(i,j,k)$, the j index runs from 0 at one end to N_k, the degree of polymerization in Kuhn lengths, at the other. Two PDF's are required to model the spatial distribution of an end-tethered polymer chain since the spatial distribution of each chain end will be different. Any arbitrary unit, j, of the chain is indexed as $q_1(i,j,k)$ by one PDF and as $q_2(i,N_k-j,k)$ by the other as shown in Figure 2. The quantity $q_n(i,j,k)$, where "n" is either 1 or 2, relates the probability of segment "j" in chain "k" on lattice layer "i" to the probability of chain end "n". The chain probability distribution functions do not give the density distributions of the polymer, but they do contain the information necessary to calculate them. A discrete diffusion equation may be generated which relates the probability densities of all segments to the chain end probability densities. Since two distinct PDF's are required to describe a linear polymer chain :

4

$$q_1(i,j,k) = \{\tfrac{1}{6}q_1(i-1,j-1,k) + \tfrac{1}{6}q_1(i+1,j-1,k) +$$
$$\tfrac{4}{6}q_1(i,j-1,k)\} \exp(-w(i,k)/kT) \qquad (1)$$

$$q_2(i,j,k) = \{\tfrac{1}{6}q_2(i-1,j-1,k) + \tfrac{1}{6}q_2(i+1,j-1,k) +$$
$$\tfrac{4}{6}q_2(i,j-1,k)\} \exp(-w(i,k)/kT) \qquad (2)$$

where $w(i,k)/kT$ is the local mean field. These discrete difference formulas were shown by Shull[14] to be equivalent to the diffusion theories of Edwards[23], Helfand and others.[24-28] Shull[20] has also shown that the solution is independent of the lattice type. In order to solve these equations, the probability densities of the chain ends must be supplied as initial conditions for all lattice layers. For an end-tethered brush, one end (the definition of whether end #1 or end #2 is adsorbing is arbitrary here) has a probability of zero everywhere except at the surface ($i = 1$) while the free end probability distribution is equal throughout the lattice for all chains.

From the chain probability distribution functions one can calculate the volume fraction of interest. The volume fraction of segment "j" of chain "k" on lattice layer "i" is given as:

$$\phi_k(i,j) = \exp(\mu_k)\, q_1(i,j,k)\, q_2(i,N_k-j,k) \qquad (3)$$

where μ_k is the chemical potential of chain "k". One obtains the total volume fraction for chain "k" by summing the segmental volume fractions over all segments j:

$$\phi_k(i) = \exp(\mu_k)\sum_{j=0}^{N_k}\{q_1(i,j,k)\, q_2(i,N_k-j,k)\} \qquad (4)$$

5

Note that the index runs from 0 to N_k, the number of Kuhn statistical segment lengths in chain "k", and that a degree of polymerization of zero is possible.

The equations which define the mean-field may be derived from Flory-Huggins thermodynamic relations. Following Shull and Kramer[29], we define the free energy density for a system of "k" distinct polymer chains as

$$F/T = \sum_k \frac{\phi_k}{N_k} \ln(\phi_k) + \frac{1}{2} \sum_m \sum_n \phi_m \phi_n \chi_{mn} \tag{5}$$

The chemical potentials, μ_k, and the mean fields, $w(i,k)$, are derived from the free energy density using the relations

$$\mu_k/N_k = \frac{\partial}{\partial \phi_k}[F/T] + F/T - \sum_k \phi_k \frac{\partial}{\partial \phi_k}[F/T] \tag{6}$$

$$w(i,k) = \mu_k/N_k - \frac{1}{N_k} \ln \phi_k(i) + \Delta w(i) \tag{7}$$

which lead to the expressions

$$\mu_k/N_k = \frac{1}{N_k} + \frac{\ln \phi_k}{N_k} - \sum_m \frac{\phi_m}{N_m} + \sum_m \chi_{mk} \phi_m - \frac{1}{2} \sum_m \sum_n \phi_m \phi_n \chi_{mn} \tag{8}$$

$$w(i,k) = \frac{1}{N_k} - \sum_m \frac{\phi_m(i)}{N_m} + \sum_m \chi_{mk} \phi_m(i) - \frac{1}{2} \sum_m \sum_n \phi_m(i) \phi_n(i) \chi_{mn} + \Delta w(i) \tag{9}$$

6

The Δw term is included in the mean field only to insure that all volume fractions sum to unity on each lattice layer (incompressible lattice). Since the volume fractions, as expressed by the equations presented here, form a monotonic function in Δw, one can use root bracketing and interval bisection techniques to find the Δw for which $\sum_k \phi_k = 1.0 \pm \epsilon$ for any arbitrarily small ϵ. In this way it is easy to control the accuracy in the solution at any given time during the relaxation. Use of a compressibility parameter to define Δw by

$$\Delta w(i) = \zeta \left[\sum_k \phi_k(i) - 1.0 \right] \qquad (10)$$

was found to obscure the degree of convergence which had been achieved by causing a slow oscillation in the total volume fraction. The probability distribution functions and mean-field relations are used coincidentally to find a self-consistent solution for the distribution of the chain segments across the lattice. A brief description of the method of solution used in this work is given in the Appendix.

While the mean-fields determine how the polymer is distributed across the lattice, it is the chemical potentials which govern the relative total amount of each component. It is difficult to calculate *a priori* those chemical potentials which would give rise to the desired molecular weight distribution. If the chemical potential of the matrix is fixed at some arbitrary value, however, the chemical potentials of the brush chains take on definite and finite (though unknown) values. As described by Shull and others[11,20,29], the mean-fields and chemical potentials are specified only to within a constant. Addition of a factor A_k to the mean field $w(i,k)$ is equivalent to adding a factor $N_k A_k$ to the chemical potential μ_k. Since this extra term is accommodated by the $\Delta w(i)$ term of

7

the mean field $w(i,k)$, the chemical potential μ_k can be changed at will to alter the overall amount of chain "k" in the system. Thus, the chemical potentials need not be calculated *a priori* and can be solved for during the relaxation process.

Modeling a Polydisperse Brush

Modeling the molecular weight distribution of a real polydisperse brush formed by adsorption from solution or melt is difficult. The distribution of molecular weights in the brush is of concern only, however, since it is assumed that the brush has already been formed and that no brush chains exist in the matrix phase. No attempt has been made to model the adsorption process itself. For this work, we assumed that the molecular weight distributions of the tethered chains could be described by the logarithmic-normal (LN) distribution. The LN distribution is mathematically convenient for modeling systems of varying polydispersity since the number average molecular weight may be fixed while the weight average molecular weight is varied. Since the ratio of the brush and matrix number average molecular weights has an affect on the interfacial width[14], constraining M_n was an important consideration.

Once the number (M_n) and weight (M_w) average molecular weights were chosen and the LN distribution generated as a continuous function, a discrete representation was needed. Since the number of different chains (of dissimilar degrees of polymerization, adsorbing or non-adsorbing) which could be simultaneously modeled was limited by available computational resources, a careful discretization was critical in insuring proper representation of the LN distribution. Furthermore, the computational requirements for modeling high molecular weight

8

polymer chains made it necessary to truncate the molecular weight distribution at some maximum molecular weight. The number of discrete chains with which the molecular weight distribution of the brush would be modeled was chosen first. This varied from 10 chains for $M_w/M_n=1.2$ to 20 chains for $M_w/M_n=3.0$. The lattice model represents polymer chains as a series of connected Kuhn segments. For this reason, the molecular weights are given in multiples of the molecular weight of the Kuhn segment, M_0. Furthermore, polydispersity is independent of molecular weight so that only the relative degrees of polymerization of the brush chains are important.

The discretization was performed by a separate computer program which followed the following scheme. An upper limit, M^*/M_0, was set on the degree of polymerization (in Kuhn lengths) under consideration such that

$$\sum_{x=0}^{M^*/M_0} P(x) = 0.99 * \sum_{x=0}^{\infty} P(x) \tag{11}$$

P(x) represents the logarithmic-normal distribution, given as

$$P(X) = \frac{e^{-\sigma^2/2}}{x_0\sigma\sqrt{\pi}}e^{-(\ln x - \ln x_0)^2/2\sigma^2} \tag{12}$$

where x_0 and σ are adjustable parameters. M_n and M_w are given by

$$\overline{M_n}/M_0 = x_0 e^{\sigma^2/2} \tag{13}$$

$$\overline{M_w}/M_0 = x_0 e^{3\sigma^2/2} \tag{14}$$

An arbitrary set of molecular weights having $M(k)/M_0$ between 0 and M^*/M_0 was generated as an initial guess. The amount, $N(k)$, of each chain was calculated using the logarithmic normal distribution function for each molecular weight of the set, $M(k)/M_0$. Finally the discrete M_n and M_w were recalculated using the relationships

$$M_n/M_O = \frac{\Sigma\{ N(k)\, M(k)/M_O \}}{\Sigma N_k} \qquad (15)$$

$$M_w/M_O = \frac{\Sigma\{ N(k)\, [M(k)/M_O]^2 \}}{\Sigma\{ N(k)\, M(k)/M_O \}} \qquad (16)$$

The results were compared with the desired values of M_n/M_0 and M_w/M_0 to generate a squared-error of fit. A multidimensional minimization routine was used to continually vary each M_k until the discrete M_n and M_w were within one percent of the desired values. M_n/M_0 was fixed equal to 100 for each molecular weight distribution and M_w/M_0 was varied to give the desired polydispersity. The matrix was modeled using one chain only, as a monodisperse brush with M_n/M_0 equal to 100.

To reduce the degrees of freedom of the problem, two other criteria were used. With the logarithmic normal distribution, the ratio M_z/M_w is identical with the ratio M_w/M_n, where M_z/M_0 is calculated by

$$M_z/M_O = \frac{\Sigma\{ N(k)\, [M(k)/M_O]^3 \}}{\Sigma\{ N(k)\, [M(k)/M_O]^2 \}} \qquad (17)$$

Also, it was desired to separate each M(k) as much as possible. Both additional criteria were included in the objective function supplied to the minimization routine. In this way, it was possible to generate an evenly distributed set of molecular weights and amounts which represented the LN distribution in a discrete fashion and had a reasonable upper bound.

Once a set of molecular weights and their amounts were chosen to represent the brush molecular weight distribution, they needed to be modeled in the brush simulation. The amount of each chain in the brush, N(k), is given by

$$N(k) = \frac{\phi_k^s}{\sigma} = \frac{\exp(-\mu_k) \cdot q_1(1,0,k) \cdot q_2(1,N_k,k)}{\sigma} \tag{18}$$

where ϕ_k^s is the volume fraction of the adsorbing end of chain "k" at the surface (i=1), and σ is the grafting density, equal to $\sum_k \phi_k^s$. The quantity $q_1(1,0,k)$ is the probability density of end #1 at the grafting surface and the term $\exp(-\mu_k)$ is the local mean-field for chain k. Note that here we have assumed that end #1 is the adsorbing end. The quantity $q_2(1,N_k,k)$ is the probability density of end #1 on the grafting surface referenced to the probability density of end #2 (see Figure 2). The probability $q_2(1,N_k,k)$ has been propagated along N_k chain segments using the discrete difference formulas given by equations (1) and (2). As mentioned earlier, the chemical potentials may be changed during the simulation to adjust the molecular weight distribution of the brush. The value for each μ_k is obtained from equation (18) since each N(k) has been determined *a priori* from the discretization of the LN distribution. With everything except $q_2(1,N_k,k)$ known, we obtain new chemical potentials at each iteration by

$$\mu_k = \ln\left\{ q_1(1,0,k) \cdot q_2(1,N_k,k) / [\sigma \cdot N(k)] \right\} \tag{19}$$

11

as $q_2(1,N_k,k)$ changes. The chemical potentials slowly cease to change as the solution evolves; when the difference between iterations is below 10^{-5} to 10^{-6} percent we assume the solution to be valid.

Results

By solving for the concentration profiles of an end-tethered brush in contact with a polymeric matrix, information about the interphase is gained. The interphase plays an important role in determining the useful properties of the brush-matrix system since adhesion between the substrate and the matrix now occurs in this zone. Since energetic effects are important, we have separately considered three cases in which values of χ = -0.1, 0.0 and 0.1 were used to represent systems in which attractive, neutral or repulsive brush-matrix interactions exist. The large repulsive enthalpic interaction is meant to represent incompatible brush and matrix polymers. The neutral enthalpic interaction represents tethered polymer in contact with a matrix of the same molecular architecture. The effect of a large attractive enthalpic interaction on the interphase was also examined. This represents the case where the brush differs from but is highly miscible with the matrix polymer. The grafting density, σ, was equal for all systems to minimize the number of variables to be explored. A value of σ=0.1 was chosen to approximate monolayer brush thickness. Since the grafting density, equal to the total volume fraction of chain ends at the surface, can be interpreted as an area per chain end there are an average of 10 square Kuhn lengths (β) surface per chain end. For a random flight chain of degree of polymerization, N, equal

to 100β, the radius of gyration, given by $R_g = \sqrt{N/6}\,\beta$, is equal to 4.08β. The exact relation

between R$_g$ for a free chain in the bulk and that for an unstretched, end-adsorbed chain is

unknown. If, however, we assume that the surface are per chain scales as R$_g^2$, we can say that the

grafting density is above the concentration for chain overlap on the surface since Rg^2 > 10β^2.

The concentration profile of a monodisperse brush is shown in Figure 3 for each of the

three enthalpic interactions, illustrating the effect which enthalpic interaction can have on the

width of the interphase. The repulsive interaction has caused the brush and matrix to demix,

sharpening the interfacial concentration profile ("dry" brush). The attractive interaction causes

the brush and matrix phases to maximize contact and swell into the matrix, reducing the

concentration gradient ("wet" brush). The athermal interaction concentration profile lies midway

between these two cases. Note that the composition at the surface (lattice layer 1) decreases from

1.0 for the repulsive interaction to approximately 0.85 for the attractive interaction. The

significance of this zone of high brush concentration near the grafting surface will be discussed in

terms of the adhesive properties of the brush-matrix system in a later section.

The discrete brush molecular weight distributions generated from the LN distributions and

used to generate the polydisperse brush profiles are shown in Table 1. The corresponding brush

concentration profiles are shown as a function of polydispersity in figures 4 ($\chi = 0.1$), 5 ($\chi = 0.0$)

and 6 ($\chi = -0.1$). Though these figures clearly show that mixing of the brush and matrix increases

with brush polydispersity, a more objective means for comparing the extents of mixing was

desired. Since the adhesive properties were of interest and since chain entanglement is the

controlling factor at a polymer-polymer interfaces, a means for measuring the entanglement

probability was desired. It was hypothesized that local entanglements are proportional to the

local volume fraction of both the brush and matrix. Stated mathematically, on lattice layer "i" entanglement density ~ $\phi_{brush}(i) \cdot \phi_{matrix}(i)$. By integrating over the entire system the overall entanglement probability can be measured. The function has the following form

$$EPF = \int \phi_{brush}(i)\left(1 - \phi_{brush}(i)\right) di \tag{20}$$

This equation shall be referred to as the entanglement probability function (EPF). This func form was chosen so that any arbitrary change in the shape of the concentration profile across the interphase could be detected, however no considerations have been made of the distance between entanglements. It is presented only as a first approximation. The entanglement probability function was calculated for each system. The results are summarized in Table 2 and plotted as a function of polydispersity, as shown in Figure 7. At a brush polydispersity of 3.0, an 82 percent increase in the EPF compared to the monodisperse brush is seen for the athermal system while an increase of 55 percent is seen for the attractive system.

Discussion

The magnitude of the change in the shape of the concentration profile with polydispersity depended upon the enthalpic brush-matrix interaction. For the values of χ studied here, the concentration profiles and EPF values were influenced by the brush polydispersity for the athermal ($\chi = 0$) and attractive ($\chi = -0.1$) enthalpic interactions only (Figure 5 and 6 respectively). The shape of the concentration profile has two distinguishing features at higher polydispersities for these systems. The brush concentration near the grafting surface in the polydisperse brush is

14

less than in the monodisperse brush and a long "foot" extends into the matrix phase. These features indicate an increase in mixing between the brush and matrix. More significantly, the "foot" indicates the extension of the longer chains into the matrix. This may indicate that higher concentrations of the longer chains will lead to ever greater EPF values.

The repulsive interactions caused the brush to collapse and sharpened the interface, resulting in a symmetric (about $\phi_{brush} = 0.5$) concentration profile. The fact that the interphase width was not influenced by brush polydispersity suggests that the repulsive interaction overwhelmed other forces which encourage mixing. One should note, however, that the values for the Flory-Huggins interaction parameter which were chosen for this study represent points within a continuum. Therefore, one would expect that intermediate values of χ would result in EPF values which, in general, follow that same trends as the three values studied here, namely an asymptotic increase in the EPF value with polydispersity. Similarly, the magnitude of the EPF increase will also depend upon χ, though for strongly repulsive systems (eg. $c \geq 0.1$) polydispersity effects should be minimal since the enthalpic interactions dominate.

Since interphase broadening is observed for the athermal system, driving forces other than enthalpic energy must be involved. Could the entropy of mixing between the brush and matrix reduce the free energy and promote mixing at high polydispersity? To further investigate this hypothesis, the free energy change of mixing for varying degrees of polydispersity were examined. The free energy change for an athermal, polydisperse system is given by

$$\Delta G_{\chi=0} = -\Delta S = \int_0^\infty \phi(M) \frac{\ln[\,\phi(M)\,]}{M} \, dM \tag{21}$$

15

where the volume fractions are specified by the logarithmic-normal distribution. This equation was integrated numerically for several values of polydispersity between 1.0 and 3.0 and various brush volume fractions. The results, shown in Figure 8, show that the free energy decreases asymptotically as polydispersity increases. Thus, the brush becomes more "miscible" with the matrix as polydispersity is increased. The effect is most pronounced between $M_w/M_n = 1.0$ and $M_w/M_n = 1.4$. Increasing polydispersity beyond 1.5 causes little change. A similar trend is observed for the EPF values, suggesting that entropic effects are linked to interfacial broadening. Since interphase broadening occurs for $M_w/M_n > 1.5$, entropic effects can, at best, only partially explain the results. To include all the molecular weights which make up the brush when calculating the overall free energy of mixing between the brush and matrix is not strictly correct, because the compositions of the brush and matrix phases vary with distance from the surface. However, the overall brush molecular weight distribution does approximate the distribution of molecular weights within the proximal (near the grafting surface) region of the brush. Therefore, while we cannot be certain that an entropically driven decrease in ΔG occurred in all parts of the brush for the athermal polydisperse system, the enhanced mixing which occurs in the proximal region may be explained by this hypothesis.

In addition to energetic considerations, one must also consider how the changing distribution of molecular weights in the brush affects the shape of the concentration profile. At polydispersities greater than 1.5, two changes occur in the molecular weight distribution of the brush.

• A high molecular weight tail begins to appear. Although these high molecular weight chains are at a low overall concentration, they represent a high proportion of the total brush

concentration in the region of the brush most distant from the surface. This could explain the presence of the "foot" which appears in the brush concentration profile, seen on lattice layers greater than 30 in Figures 5 and 6.

• As the molecular weight distribution broadens, the concentration of species having $M \sim M_n$ is decreasing while the concentration of species in which $M \ll M_n$ and $M \gg M_n$ is increasing. This may contribute to the reduction in the total brush concentration in the central region of the brush observed in Figures 5 and 6.

These effects work in tandem to extend the brush into the matrix and broaden the width of its interphase. Thus, the shape of the concentration profile may be affected to some degree by the shape of the distribution of molecular weights in the brush. Because entropic effects can never be "turned off", however, this is difficult to prove. Still, since the shape of the concentration profile directly affects the interpenetration of the brush and matrix phases, it also affects their adhesion and response to stress. With this result in mind, it seems natural to ask the question "Can the molecular weight distribution be specified so that the interphase width is maximized or tailored to fit a particular need"? The impact of the answer would be far-ranging and will be left to a forthcoming paper.

Adhesive Properties

The interfacial concentration profile of the brush can be used to infer how the adhesive properties of the interphase are affected by polydispersity. Of particular interest is the interfacial toughness. Several papers[9,10,30-33] on the problem of polymer-polymer adhesion have recently been published. We are primarily concerned with the adhesion between the brush and matrix. This is

essentially a polymer-polymer adhesion problem even though the brush is tethered to the solid. Raphael and deGennes[30] considered the fracture of the "weak mechanical junction" consisting of two rubber phases which are joined essentially by a polymer brush which is grafted to the surface of one rubber phase and which penetrates into the other phase only. The geometry of our model is similar to that used in their paper in the sense that one phase is impenetrable by the polymer brush chains. The authors found that the interfacial toughness, G, scales as the degree of polymerization, N_k. This relationship was predicted to occur in the limit of very small grafting density, where the chains were isolated from each other. Brown[9] and Creton and Brown[10] studied the chain pullout of the elastomeric segment of a diblock copolymer from a crosslinked rubber lens, analogous to the geometry of the Raphael and deGennes model. Their results confirmed a first order dependence of G on N at low crack velocities ($\sim 10^{-9}$m/s), however, the exponent was found to decrease slightly as the degree of polymerization of the elastic segment increased.[10] One explanation given by the authors for this observation considered the miscibility between the rubber lens and the penetrating copolymer block. They suggested that, as the molecular weight of the block increased, entropy favored demixing such that the monomeric friction factor was effectively reduced.

We would like to postulate that a consideration of the brush structure gives rise to an alternate explanation for the observed less than linear dependence of G on N. Consider a planar surface which has a brush at low grafting density in contact with a polymeric matrix. For low N of the brush, the chains would be isolated from each other and the number of matrix-surface contacts would be of the same order as brush-surface contacts. As N increases, the brush chains would begin to touch each other and cover the surface. At still higher N, the matrix would be

18

excluded from a zone near the surface. The near-surface brush chain segments would have little

contact with the matrix polymer and could not contribute to the total resistance of the brush to

stress. This reduces the effective molecular weight of the brush which is available for chain

pullout or other energy dissipation mechanisms which contribute to the overall toughness, causing

the N dependence to be weaker than that predicted by the model of Raphael and deGennes. This

effect has been considered previously[32] where an effective entanglement density was calculated for

a diblock copolymer at the interface between two immiscible polymer phases. We maintain that,

when an exclusion zone is present, the effective number of chain segments which can contribute

to G is limited to those segments which actually penetrate the matrix phase (eg., the lens). In light

of this result, we conclude that a consideration of the brush-matrix interphase is important when

estimating the contribution of chain pullout to the interfacial toughness.

This consideration is naturally included in the mathematical form of the EPF which

essentially qualitatively measures the degree of mixing between the brush and matrix. We

postulate that one brush segment must contact one matrix segment to create an effective contact

which will contribute to chain pullout and that the EPF essentially measures an overall

segment-segment contact probability. The toughness of each system can then be ranked

according to its EPF (Figure 7 and Table 2). It is important to note that we have assumed that

the interface is purely diffuse. This is consistent with the initial assumption that the system was

isotropic in all directions except that perpendicular to the interface. Thus we have shown that

increasing the polydispersity of an end-tethered brush increases the adhesion between it and a

polymeric matrix with which it is in contact, at least in the limit of low crack speeds. In any case,

for systems in which the strength of the interphase is weak and adhesive failure dominates, we

19

expect adhesion to increase with polydispersity in general. Experiments to verify these results are currently underway.

The adhesive bond will fail at its weakest point. If the goal is simply to maximize the EPF value this can easily be achieved by using a high molecular weight brush at low grafting density. If the brush molecular weight is continually increased and the grafting density is restricted to sufficiently small values such that the brush is always "wet" then the EPF value should also increase continually. There is a price to be paid, however, since the weakest point has now shifted from the brush-matrix *interphase* to the substrate-brush *interface* causing the overall adhesive strength to be low. One must balance the strength of the interphase (controlled primarily by entanglements) and the strength of the interface (controlled by the surface density of brush-substrate bonds) so that neither is a "weak link". Thus, the problem becomes finding a suitable molecular weight distribution (M_n, M_w and shape) which will simultaneously allow sufficiently high grafting densities and broad interphases. In order to correctly model this problem, a means for calculating the actual strengths or toughnesses for the interface and interphase must be incorporated into the SCF framework. Only then can the relationship between brush polydispersity and adhesion in substrate-brush-matrix systems be properly addressed.

Conclusions

A self-consistent field computer simulation has been used to calculate the concentration profile of an end-tethered polymer chain in a polymer matrix in order to investigate the influence of brush polydispersity on the width of the interphase. Systems having athermal, attractive and repulsive brush-matrix enthalpic interactions were investigated separately. It was found that

increasing the degree of polydispersity of the brush increased the width of the interphase between the brush and matrix. Enthalpic effects largely governed the degree of interfacial broadening brought on by an increase in polydispersity such that no significant broadening was observed for a repulsive interaction. Interphase broadening was thought to arise from two forces which acted independently on near surface (proximal), central and distal (exterior) regions of the brush. The enhanced mixing in the proximal region was attributed to entropic effects by showing that the free energy of mixing decreased in an asymptotic fashion as polydispersity increased. The extension of the distal portion of the brush into the matrix in the form of a "foot" of low concentration was thought to arise from the presence of long chains in the brush molecular weight distribution. The reduction of the concentration gradient in the central region of the brush was also attributed to a redistribution of the chain lengths away from M_n as polydispersity increased.

The implications of the simulation results on the adhesive properties of the brush-matrix interphase were also discussed. It was observed that an exclusion zone in the proximal region of the brush may arise under certain conditions, reducing the effective molecular weight of the brush and, therefore, the toughness of the interphase. It was also determined that the number of brush-matrix contacts increases in the same manner as the interphase width given by the entanglement probability function. An increase in the toughness of the brush-matrix interphase of 50 percent (attractive), 82 percent (athermal) and 3 percent (repulsive) for was predicted for a polydispersity of 3.0 as compared to the monodisperse brush. This demonstrates that highly polydisperse brush architectures can be used to enhance the adhesion of a substrate to a polymeric matrix provided that the enthalpic interactions are not highly repulsive in nature.

Acknowledgements

Appendix I : Method of Solution

An iterative relaxation scheme was followed to find a self-consistent solution to the PDF's. An arbitrary initial guess was made for the probability distribution functions and mean fields across the entire lattice. The recursion relations (eqns. 1, 2) were then used to recalculate the PDF's for the first lattice layer. The chemical potentials were then recalculated to insure the correct amount of each chain in the brush (N(k)). Next, the volume fractions were made to sum to unity by adjusting the Δw term of the mean-fields as explained in the text. Finally the mean fields were recalculated using the normalized volume fractions. The PDF's for the remaining lattice layers could then be recalculated using equations (1) and (2), the volume fractions normalized and the mean fields recalculated as on the first lattice layer.

Recalculating the PDF's for all lattice layers constituted one iteration. The changes in the volume fractions and chemical potentials on each lattice layer with respect to the values held at the end of the previous iteration were evaluated and the maximum change in each was found. These values were compared with the tolerances set at the beginning of the program to see if convergence had been achieved. Typically, when the maximum change per iteration was less than 10^{-5} percent for the chemical potentials and 10^{-6} for the volume fractions, it was assumed that the self-consistent solution had been reached.

The number of iterations required before the convergence criteria were met varied from approximately 500 iterations for a monodisperse, athermal system to 10,000 to 20,000 iterations for a non-athermal system having a polydispersity index of 3.0 (20 chains, maximum value for $M/M_0 = 2000$). The largest simulations required approximately 20 hours on an Stardent Systems Model 1500 computer using 4 MIPS 3000 CPU chips operating in parallel.

Bibliography

1. Madhukar, M.; Drzal, L.T. J.Comp.Mat. **1992**, *26*, 310.

2. Madhukar, M.; Drzal, L.T. J.Comp.Mat. **1991**, *25*, 958.

3. Madhukar, M.; Drzal, L.T. J.Comp.Mat. **1991**, *25*, 932.

4. Madhukar, M.; Drzal, L.T. J.Comp.Mat. **1992**, *26*, 936.

5. Gent, A.N.; Petrich, R.P. Proc.Roy.Soc. **1969**, *A310*, 433.

6. Orowan, E. J.Franklin Instit. **1970**, *290*, 293.

7. Gent, A.N.; Kinloch, A.J. J.Poly.Sci. **1971**, *A-2*, 9, 659.

8. Napolitano, M.J.; Moet, A. J.Adhesion **1991**, *33*, 149.

9. Brown, H.R. IBM research report #RJ 9077 (80890), **1992**.

10. Creton, C.; Brown, H.R. prepublication manuscript.

11. Hong, K.M.; Noolandi, J. Macromolecules **1980**, *14(3)*, 727.

12. Scheutjens, J.M.H.M.; Fleer, G.J. J.Phys.Chem. **1980**, *84(2)*, 178.

13. Leibler, L. Macromolecules **1980**, *13*, 1602.

14. Shull, K. J.Chem.Phys. **1991**, *94(8)*, 5723.

15. (a) Dan, N.; Tirrell, M. Macromolecules **1992**, *25*, 2890. (b) Ji, H.; Hone, D.
    Macromolecules **1988**, *21*, 2600. (c) Kawaguchi, M.; Anada, S.; Nishikawa, K.; Kurata,
    N. Macromolecules **1992**, *25*, 1588. (d) Ji, H.; Hone, D.; Pincus, P.A. Macromolecules
    1987, *20*, 2543.

16. (a) Milner, S.T.; Witten, T.A.; Cates, M.E. Macromolecules **1988**, *21*, 2610. (b) Klein, J.; Dvora, P.; Warburg, S. Nature **1991**, *352*, 143. (c) Kumaran, V. Macromolecules **1993**, *26*, 2464. (d) Klushin, L.I.; Svortsov, A.M. Macromolecules **1991**, *24*, 1549.

17. Milner, S.T.; Witten, T.A.; Cates, M.E. Macromolecules **1989**, *22*, 853.

18. Tirrell, M. ACS Conference on Surfaces and Interfaces, Oct. 21, 1992, Danvers, Mass.

19. Cosgrove, T.; Heath, T.; Van Lent, B.; Leermakers, F.; Scheutjens, J. Macromolecules **1987**, *20*, 1692.

20. Shull, K. Macromolecules **1992**, *25*, 2122.

21. Yeung, C.; Balazs, A.C.; Jasnow, D. Macromolecules **1993**, *26*, 1914.

22. Huang, K.; Balazs, A.C. Macromolecules **1993**, *26*, 4736.

23. Edwards, S.F. Proc.Phys.Soc.London **1965**, *85*, 613.

24. Helfand, E.; Wasserman, Z.R. Macromolecules **1976**, *9*, 879.

25. Helfand, E.; Tagami, Y. J.Chem.Phys. **1972**, *57*, 1812.

26. Helfand, E.; Sapse, A.M. J.Chem.Phys. **1975**, *62*, 1327.

27. Noolandi, J.; Hong, K.M. Macromolecules **1982**, *15*, 482.

28. Noolandi, J.; Hong, K.M. Macromolecules **1984**, *17*, 1531.

29. Shull, K.R.; Kramer, E.J. Macromolecules **1990**, *23*, 4769.

30. Raphael. E.; deGennes, P.G. J.Phys.Chem. **1992**, *96*, 4002.

31. Ji, H.; deGennes, P.G. Macromolecules **1993**, *26*, 520.

32. Washiyama, J.; Kramer, E.J.; Hui, C-Y. Macromolecules **1993**, *26*, 2928.

33. Creton, C.; Kramer, E.J.; Hui, C.; Brown, H.R. Macromolecules **1992**, *25*, 3075.

Figure and Table Captions :

Table I - The discrete molecular weight distributions obtained from the logarithmic-normal distribution function.

Table II - Summary of EPF values, showing the percent increase over the monodisperse value.

Figure 1 - Cubic lattice arrangement showing the six nearest neighbor positions. Note all five atoms lying in the solid plane are within the same lattice layer and considered equivalent.

Figure 2 - Illustration of the indexing scheme for the probability distribution functions. The index j denotes the distance along the backbone, away from a particular chain end, that a segment is located. Note that two probability density functions are used to model one chain.

Figure 3 - Brush profiles for a monodisperse brush having an attractive, neutral or repulsive brush-matrix enthalpic interaction.

Figure 4 - Brush profiles for the case of repulsive interaction. Note that polydispersity shows no influence on the width of the interphase.

Figure 5 - Brush profiles for for the case of neutral interaction. The arrows indicate the direction of increasing polydispersity.

Figure 6 - Brush profiles for for the case of attractive interaction. The arrows indicate the direction of increasing polydispersity.

Figure 7 - EPF values for athermal (upper curve), attractive (middle curve) and neutral (lower curve) interactions. Note that a continuum exists between the values shown.

Figure 8 - Free energy given by equation 21 as a function of polydispersity. The results are shown for overall brush volume fractions of 0.1 (shaded squares), 0.25 (shaded triangles), 0.5 (asterisks), 0.75 (open squares) and 0.9 (crosses).

Table I - Discretized, Log-Normal Molecular Weight Distributions Employed in Simulations

Mw/Mn = 1.2		Mw/Mn = 1.4		Mw/Mn = 1.6	
M(k)/Mo	N(k)	M(k)/Mo	N(k)	M(k)/Mo	N(k)
36	0.021013	30	0.044803	20	0.025197
51	0.089124	44	0.117125	31	0.073994
64	0.15976	78	0.218509	44	0.130461
79	0.213198	61	0.188369	83	0.187511
98	0.222677	104	0.206941	66	0.181579
127	0.167429	149	0.136816	102	0.175439
170	0.078199	225	0.053072	134	0.139791
212	0.03222	288	0.023635	254	0.04413
260	0.011192	386	0.007157	323	0.022849
295	0.005188	447	0.003574	403	0.01118
				498	0.005119
				580	0.002749

Mw/Mn = 1.8		Mw/Mn = 2.0		Mw/Mn = 3.0	
M(k)/Mo	N(k)	M(k)/Mo	N(k)	M(k)/Mo	N(k)
13	0.014803	11	0.012423	12	0.037908
25	0.0718	31	0.092437	22	0.076301
40	0.142519	40	0.11945	32	0.099469
62	0.192511	54	0.143251	43	0.112037
76	0.198081	67	0.150647	56	0.116504
103	0.181273	87	0.146355	68	0.115141
159	0.121599	112	0.129601	84	0.109329
279	0.045014	229	0.055752	106	0.098528
368	0.022647	133	0.113198	132	0.085381
596	0.005015	413	0.015963	172	0.067762
687	0.002982	493	0.009942	220	0.051617
787	0.001757	617	0.005114	435	0.018215
		726	0.003017	830	0.004593
		854	0.001716	1073	0.002391
		956	0.001133	1266	0.001521
				1424	0.001086
				1597	0.000772
				1750	0.000584
				1877	0.000468
				1982	0.000394

Table II - Entanglement Probability Function summary

Athermal	Mw/Mn	EPF	percent increase
	1	2.159	---
	1.2	2.679	24.1
	1.4	3.012	39.5
	1.6	3.245	50.3
	1.8	3.438	59.2
	2	3.56	64.9
	3	3.937	82.4

Repulsive	Mw/Mn	EPF	percent increase
	1	1.106	---
	1.2	1.124	1.6
	1.4	1.129	2.1
	1.6	1.129	2.1
	1.8	1.130	2.2
	2	1.130	2.2
	3	1.132	2.4

Attractive	Mw/Mn	EPF	percent increase
	1	3.598	---
	1.2	4.382	21.8
	1.4	4.752	32.1
	1.6	4.958	37.8
	1.8	5.164	43.5
	2	5.248	45.8
	3	5.577	55.0
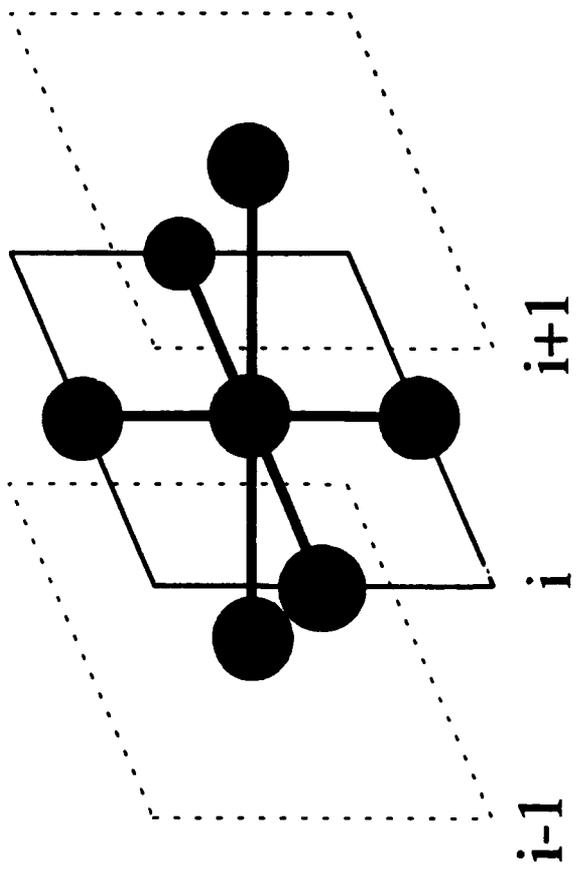
Figure 1

Figure 2

FIGURE 3

repulsive interaction

attractive interaction

neutral interaction

lattice layer

brush volume fraction

FIGURE 4

brush volume fraction (y-axis): 0, 0.2, 0.4, 0.6, 0.8, 1

lattice layer (x-axis): 0, 10, 20, 30, 40, 50, 60
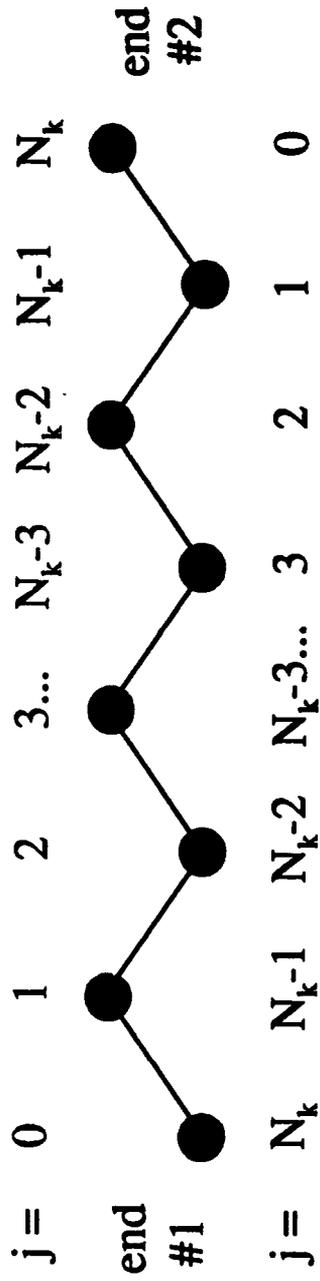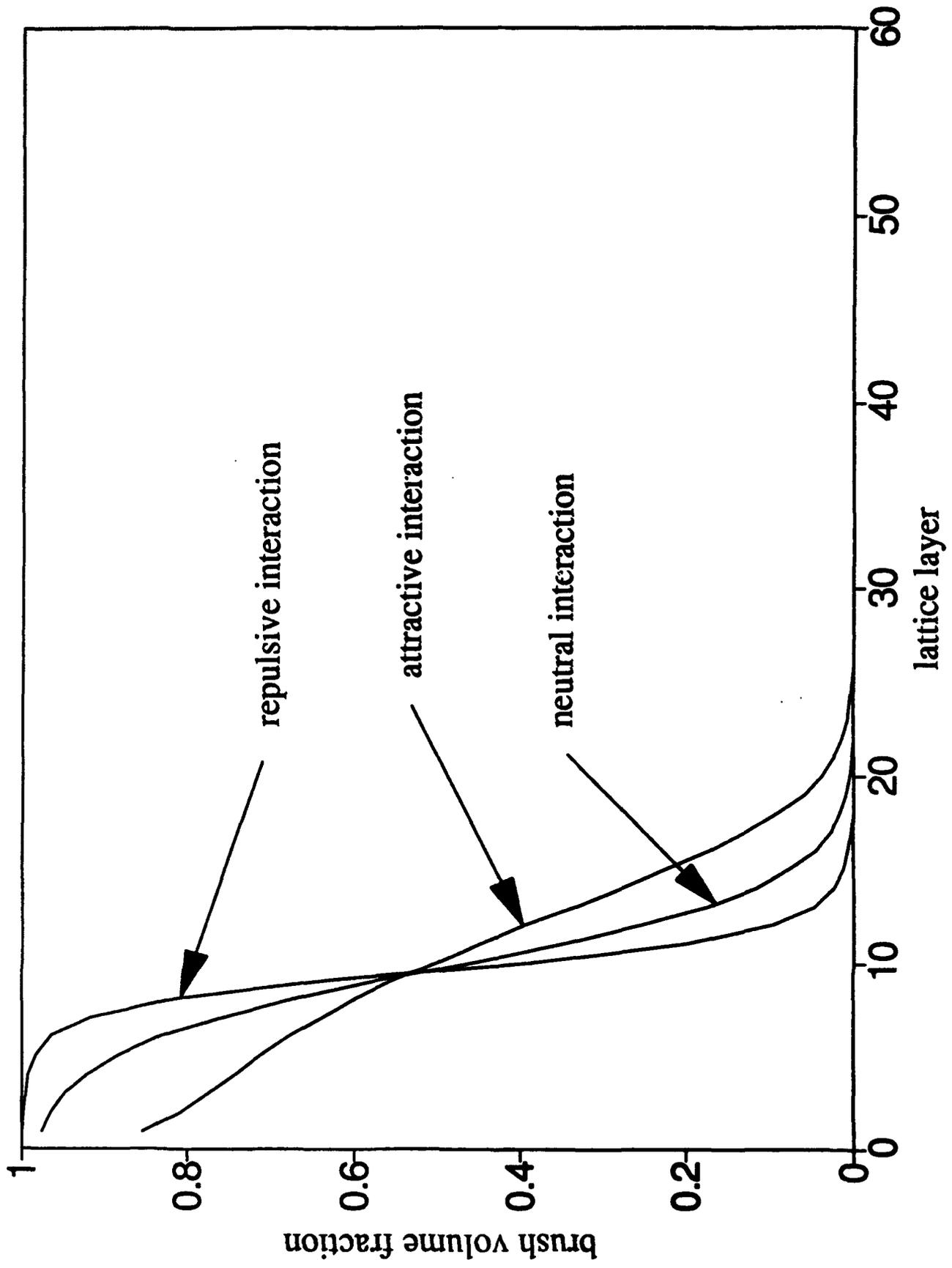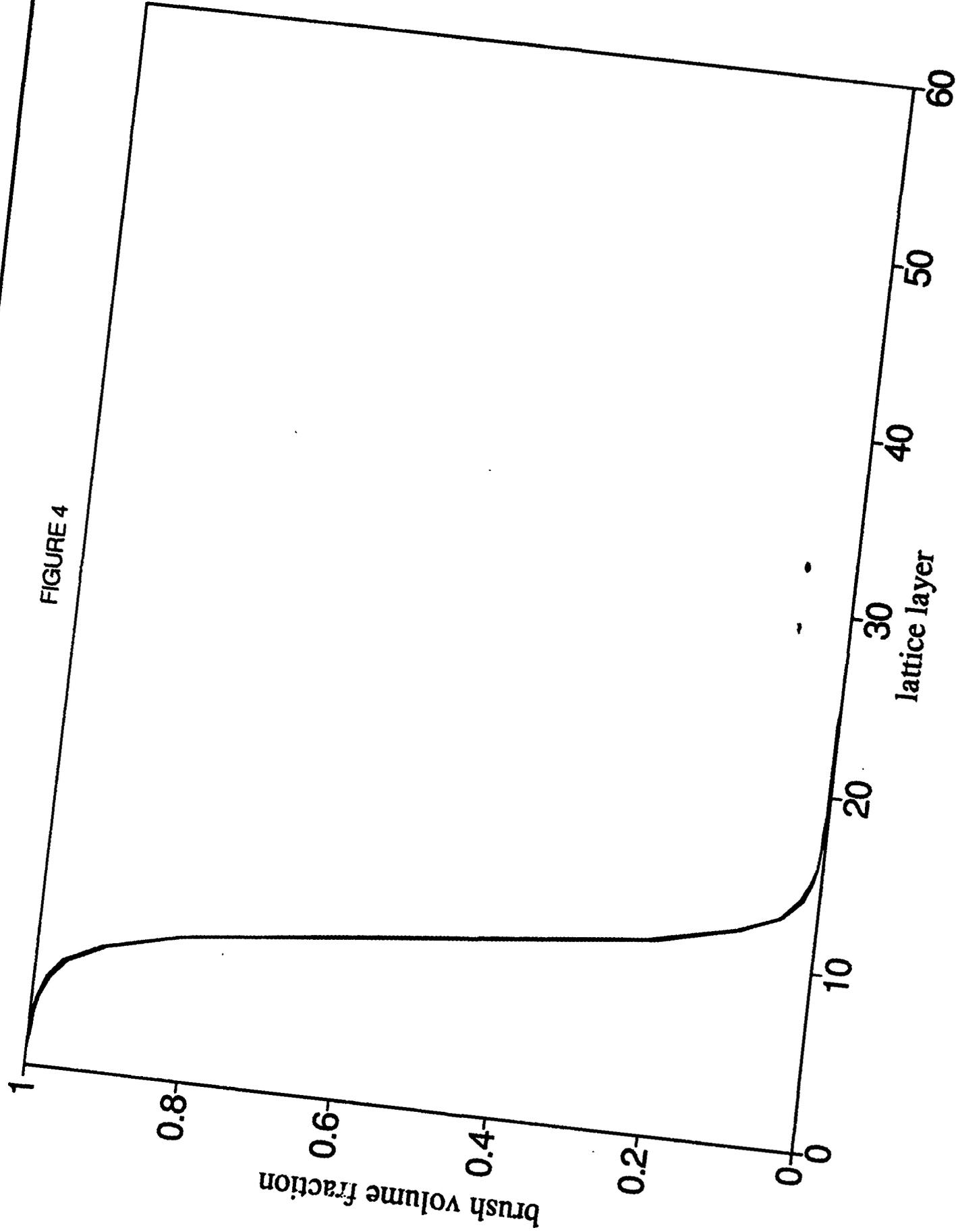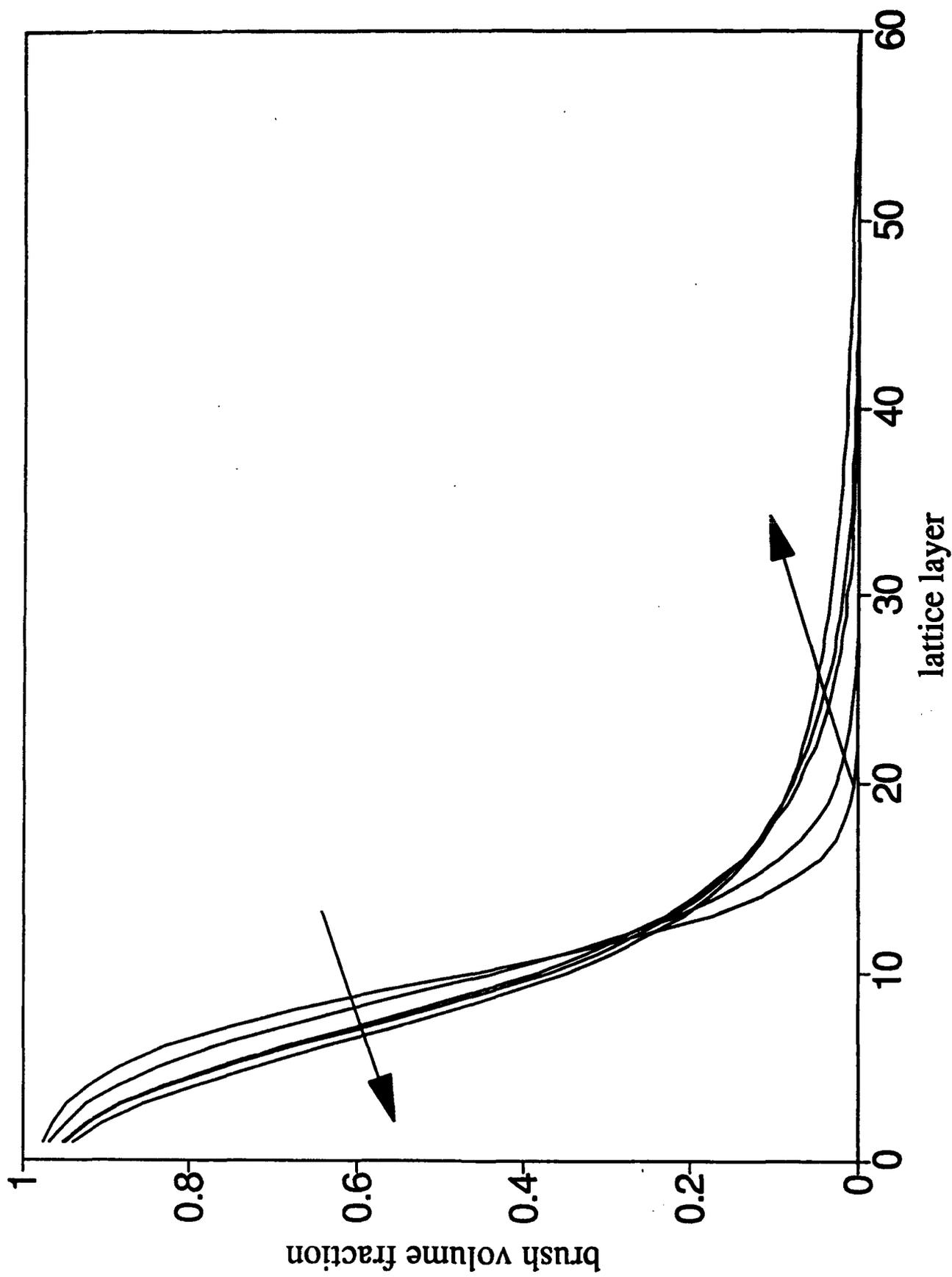
FIGURE 5

FIGURE 6

FIGURE 7

FIGURE 8